Correlation of charged fluids separated by a wall of finite thickness: Dependence on the charge of the fluid and the wall

Marcelo Lozada-Cassou and Jiang Yu
Departamento de Física, Universidad Autónoma Metropolitana–Iztapalapa, Apartado Postal 55-534, 09340 México, Distrito Federal, Mexico
(Received 9 December 1996)

It is shown that a charged fluid in contact with a planar electrode, of finite thickness, is correlated with the charged fluid on the other side of the electrode. Results for several plate and fluid parameters are presented. Thicker electrical double layers seem to promote a stronger correlation between the liquids at both sides of the wall. [S1063-651X(97)04209-8]

PACS number(s): 61.20.Qg, 61.20.Gy

I. INTRODUCTION

If a charged fluid is next to a charged electrode of planar geometry, a charge concentration profile is induced on the fluid next to the plate. This charge concentration profile has a maximum at the point of contact with the plate and decreases as it moves away from the plate, to reach its minimum value of zero in the bulk fluid. This charge profile is known as the electrical double layer (EDL) in the liquid and colloidal dispersion fields. Since the classical work of Gouy [1] and Chapman [2] it has been universally accepted that the EDL formed by a charged fluid next to a planar, charged electrode is independent of the fluid that might be on the other side of the electrode. For example, this has been the case in liquid theory studies [3–14], numerical simulations [15–17], and classical monographs and textbooks on colloids [18–26]. To the best of our knowledge, all the literature in the field assumes either that there is no correlation between the fluids on both sides of the dividing wall or that the wall is infinitely thick.

The Poisson-Boltzmann equation [1,2] or theories based on charge moment expansions [3] simply do not include proper boundary conditions in order to take into account the fluid on the other side of the wall. From the point of view of the integral equation theories, the reason for this approach is probably due to the influential work of Henderson, Abraham, and Barker [4] and that of Henderson and Blum [5]. In these papers a method for deriving integral equations for inhomogeneous fluids is proposed. In this method the Ornstein-Zernike (OZ) equation [4] for an $(n+1)$-component homogeneous fluid is generalized to study inhomogeneous fluids. The limits of infinite radius and zero concentration for the $n+1$ species is taken in the OZ equation and the other n species are left as the liquid species. Hence the field produced by the giant particle (assumed to be spherical) becomes the source of the external field and thus produces an inhomogeneity in the fluid. Because this central particle is giant, the fluid near it ''sees'' it as a planar wall. Let us refer to this method as the asymptotic method (AM) [27]. A shortcoming of this method is that it is restricted to planar, infinitely thick walls. As we will show later, with a wall of infinite thickness there is no liquid-liquid correlation through the wall.

The equivalence between particles and fields is well established in physics, i.e., particles and fields are defined through their interactions with other particles or external fields. The various microscopic liquid theories are basically mathematical manipulations of the species probability densities, starting from a conservation equation or a probability density ansatz. Since there are no restrictions in these statistical mechanical theories in relation to the type of the particles' interaction potential, the number of species in a fluid, and their concentrations, one can consider the external field in an inhomogeneous fluid to be just another particle in a homogeneous fluid. This very simple idea was used in the past by one of us to propose a method to derive theories for inhomogeneous liquids [27]. We will refer to this method as the direct method (DM). This method has been applied successfully to study inhomogeneous liquids next to external fields of several geometries [28]. The DM allows the study of an inhomogeneous fluid next to an electrode of *any shape and size*, in particular that of an electrode of planar geometry and a *finite* thickness. Apparently there is some confusion in the literature with regard to the differences between the DM and the AM [29]. Clearly the DM is more general than the AM, but it is *not* a generalization of the AM: The AM is a mathematical procedure to deal with the fluid structure around a very large spherical particle in the fluid [4]. Hence the AM can be applied only to the particular case of an infinitely thick, wide, and long plate. The DM is based on the well-established equivalence between particles and fields and can be applied to fluids in external fields of any size and shape. The AM is a geometrical limit and the above equivalence does not seem to have been recognized. If the equivalence between particles and fields is recognized the mathematical limit is clearly unnecessary [27,28]. The AM can be obtained from the DM, the opposite is not true.

In a recent Letter [30] we showed that a correlation exists between charged fluids separated by a charged wall of finite thickness. Here we study the extent of this effect as a function of the plate and liquid parameters. In Sec. II we outline the derivation of the hypernetted-chain–mean-spherical approximation (HNC-MSA) equation for a finite plate. The HNC-MSA integral equation theory has been shown to be a successful theory for infinitely thick charged plates [7,15]. In Sec. III we present our results. In Sec. IV we give some conclusions.

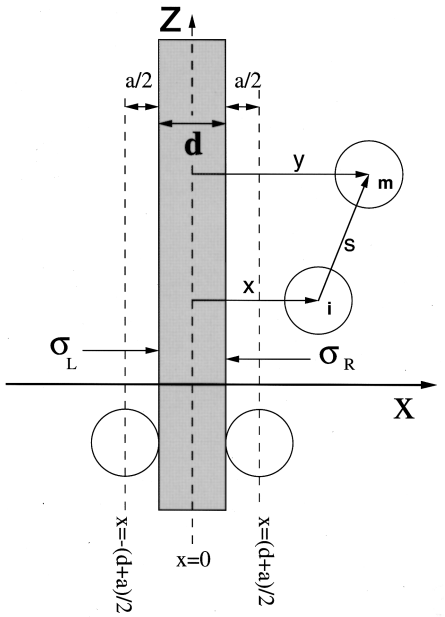

FIG. 1. Geometry for a charged plate, immersed in a restricted primitive model electrolyte.

II. THEORY

With the DM [27,28], the HNC-MSA equation for a two-component electrolyte next to the external field produced by a charged plate of thickness d is obtained in a straightforward manner, i.e.,

$$g_{pi}(x)=\exp\left\{-\beta u_{pi}(x)+\sum_{m=1}^{2}\rho_m\int c_{im}(s)h_{pm}(y)dv_3\right\}, \tag{1}$$

where ρ_m is the bulk concentration of the ions of species m; $c_{im}(s)$ is the MSA direct correlation function for ions of species i and m, a distant s apart; $\rho_i g_{pi}(x)$ is the local concentration of ions of species i, at a distance x from the center of the plate and perpendicular to the plate (see Fig. 1); $h_{pm}(y)$, defined as $h_{pm}(y)\equiv g_{pm}(y)-1$, is the total correlation function; dv_3 is the volume differential; $\beta\equiv 1/kT$, where k is the Boltzmann constant and T is the system temperature; and $u_{pi}(x)$ is the interaction potential between an ion of species i and the plate, represented by the subindex p. A widely used model for the electrolyte is the so-called restricted primitive model electrolyte. In this model the electrolyte is assumed to be a fluid of charged hard spheres of charge ez_i and diameter a, in a dielectric continuum of dielectric constant ϵ, where e is the electronic charge and z_i is the valence of an ion of species i. In this paper the plate is considered to be a flat, hard wall with a surface charge density σ_L on the left-hand side surface of the plate and a surface charge density σ_R on the right-hand side surface of the plate. The wall has a width d and is composed of a dielectric material with a dielectric constant chosen to be equal to that of the solvent, for simplicity, such that image forces need not be considered. This model for the electrode differs from others in the literature [1–26] in that the *thickness* of the plate is taken into account and its two surfaces need not be *equally* charged. As pointed out before, to the best of our knowledge, in the past this wall was explicitly or implicitly assumed to be infinitely thick.

For our model, this potential can be separated into a hard-sphere–hard-wall term $u^{*}_{pi}(x)$ and an electrostatic part $u^{\mathrm{el}}_{pi}(x)$. The hard-sphere–hard-wall potential simply takes into account the fact that the ions cannot penetrate or deform the walls. From Gauss's law the electrostatic potential can be found to be

$$-\beta u^{\mathrm{el}}_{pi}(x)=\frac{2\pi\beta ez_i}{\varepsilon}(\sigma_L+\sigma_R)x. \tag{2}$$

Equation (1) is a nonlinear integral equation that we solved numerically with advanced finite-element techniques. The solution of Eq. (1) gives the concentration profile $\rho_i g_{pi}(x)$ to the left and right of the wall.

The charge profile in the solution is given by

$$\rho_{\mathrm{el}}(x)=\sum_{m=1}^{2} ez_m\rho_m g_{pm}(x). \tag{3}$$

The electroneutrality condition for the plate plus the electrolyte system states that the charge induced in the liquid by the wall must cancel that on the wall, that is, $\sigma_L+\sigma_R=\sigma'_L+\sigma'_R$, where σ'_L and σ'_R are the induced charges in the liquid to the left and right of the plate, respectively. Mathematically this condition is expressed as

$$\sigma_L+\sigma_R=-\int_{-\infty}^{-d/2}\rho_{\mathrm{el}}(y)dy-\int_{d/2}^{\infty}\rho_{\mathrm{el}}(y)dy, \tag{4}$$

where the first and second integrals define σ'_L and σ'_R, respectively.

For an isolated charged plate the net pressure must be zero. However, for an unsymmetrically charged plate, the Maxwell stress tensor contributions to the pressure on each side of the plate will not in general be equal. Thus the kinetic stress tensor contributions must be such that the net pressure is zero. An exact expression for this net pressure can be obtained from that for the interaction of two plates, as the limit of plates' infinite separation [31,32], i.e.,

$$P=-\frac{2\pi}{\varepsilon}[\sigma'_L-\sigma'_R]+kT[\rho_s(-d/2-a/2)-\rho_s(d/2+a/2)], \tag{5}$$

where the first and second terms on the right-hand side are the Maxwell and kinetic stress tensors contributions to the net pressure and

$$\rho_s(x)\equiv\sum_{m=1}^{2}\rho_m g_{pm}(x). \tag{6}$$

As a test for our theory we have calculated the net pressure on the plate and found that indeed the Maxwell and kinetic stress tensors contributions are different on each side of the plate, but still the net pressure is zero. This result is in disagreement with that for the ideally polarizable interface model (IPIM) of Rosinberg, Blum, and Lebowitz [33,34]. They do not find a net zero pressure. We find our result more

physically appealing. The IPIM is obtained with the AM as the limit of infinite radius for two concentric spherical shells. There is fluid inside the inner shell and outside the exterior shell. There is no fluid in between the shells. Appendix D in Ref. [33] is particularly useful to compare with our model.

From the charge profile (3) the mean electrostatic potential (MEP) can be calculated. Following the derivation presented in Appendix B of Ref. [32], the MEP for a charged plate immersed in a charged fluid is obtained as

$$\psi(x)=\begin{cases} -\dfrac{4\pi}{\varepsilon}\displaystyle\int_{-\infty}^{x}(x-y)\rho_{\rm el}(y)dy, & x<-\dfrac{d+a}{2} \\ \dfrac{4\pi}{\varepsilon}\displaystyle\int_{x}^{\infty}(x-y)\rho_{\rm el}(y)dy, & x>\dfrac{d+a}{2} \end{cases} \tag{7}$$

$$\psi(x)=\frac{4\pi\sigma_L'}{\varepsilon}x+\frac{4\pi(\sigma_L'+\sigma_R')}{\varepsilon}\frac{d}{2}-\frac{4\pi\sigma_R}{\varepsilon}d-I_0, \quad -\frac{d+a}{2}<x<-\frac{d}{2} \tag{8}$$

$$\psi(x)=-\frac{4\pi\sigma_R'}{\varepsilon}x+\frac{4\pi\sigma_R}{\varepsilon}\left(x-\frac{d}{2}\right)-I_0, \quad -\frac{d}{2}<x<\frac{d}{2} \tag{9}$$

$$\psi(x)=-\frac{4\pi\sigma_R'}{\varepsilon}x-I_0, \quad \frac{d}{2}<x<\frac{d+a}{2} \tag{10}$$

where

$$I_0=\frac{4\pi}{\varepsilon}\int_{(d+a)/2}^{\infty}y\rho_{\rm el}(y)dy. \tag{11}$$

III. RESULTS

In Fig. 2 the fluid is a 2:2, 0.971M electrolyte. Several surface charge densities on the left and right surfaces of the wall were considered: (a) On its left surface $\sigma_L=0.272$ C/m^2 and on its right surface $\sigma_R=0.272$ C/m^2; (b) $\sigma_L=0.3627$ C/m^2 and $\sigma_R=0.1813$ C/m^2; (c) $\sigma_L=0$ C/m^2 and $\sigma_R=0.544$ C/m^2; (d) $\sigma_L=-0.136$ C/m^2 and $\sigma_R=0.68$ C/m^2. In all cases $\sigma_R+\sigma_L=0.544$ C/m^2. The thickness of the wall is $d=a$. In Fig. 2(a) we show the positive-ion reduced concentration profile (PIRCP), induced by the wall in the solution. In Fig. 2(b) the negative-ion reduced concentration profile (NIRCP) is shown. At the left-hand side of the wall, near the wall, the PIRCP is lower than in the bulk solution, whereas the NIRCP is clearly above its bulk value [far from the wall, i.e., in the bulk, $g_{p\_}(x)=g_{p_+}(x)=1$, since the wall's electrical field is screened by the charged fluid]. This is an unexpected behavior for cases (c) and (d) because the left-hand side of the wall has zero charge or is negatively charged, respectively. For cases (a) and (b) this qualitative behavior is to be expected since the left-hand side of the wall is positively charged. At the right-hand side of the wall an apparently normal behavior is observed near the wall, i.e., the PIRCP is lower than one and the NIRCP is well above than one. Since the right surface of the wall is positively charged, this is to be expected. These results suggest that a correlation between the left and right liquids exists since the wall-ion interaction potential is symmetric with respect to the left- and right-hand sides of the wall [see Eq. (2)].

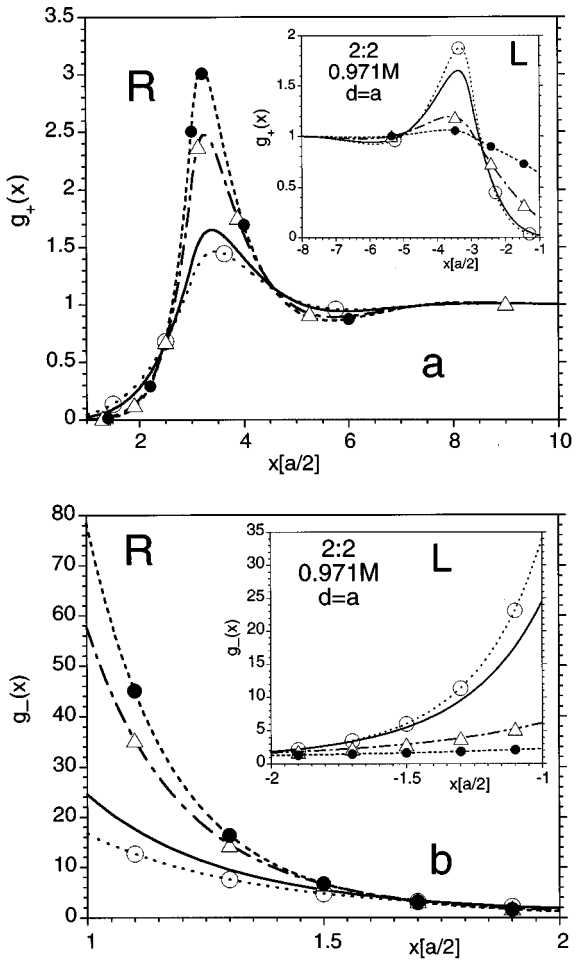

FIG. 2. Reduced concentration profiles (RCPs) for a 2:2, 0.971M electrolyte, next to a charged wall, as a function of the distance to the wall, in units of ionic radius. The wall has different surface charge densities: (a) On its left surface $\sigma_L=0.272$ C/m^2 and on its right surface $\sigma_R=0.272$ C/m^2 (solid line); (b) $\sigma_L=0.3627$ C/m^2 and $\sigma_R=0.1813$ C/m^2 (open circles); (c) $\sigma_L=0$ C/m^2 and $\sigma_R=0.544$ C/m^2 (triangles); (d) $\sigma_L=-0.136$ C/m^2 and $\sigma_R=0.68$ C/m^2 (filled circles). In all cases $\sigma_R+\sigma_L=0.544$ C/m^2. The thickness of the wall is $d=a$. In (a) we show the positive-ion reduced concentration profile (PIRCP), induced by the wall in the solution. In (b) the negative-ion reduced concentration profile (NIRCP) is shown. The distance to the wall is measured in ionic radius. The zero of the x coordinate is located on the left surface of the wall for the left RCPs and on the right surface of the wall for the right RCPs, i.e., the thickness of the wall is not plotted. The left RCPs are shown in the inset.

Case (a) is the symmetric situation, that is, the left PIRCP and the left NIRCP are equal to the corresponding right PIRCP and right NIRCP. A higher or lower surface charge density than that in case (a) produces a NIRCP, in cases (b)–(d), correspondingly, higher or lower than that of case (a) and a lower or higher PIRCP contact value. Does this means that the charge induced in the liquids at the left and right of the wall are equal to the corresponding, given surface charge densities on the left and right faces of the wall?

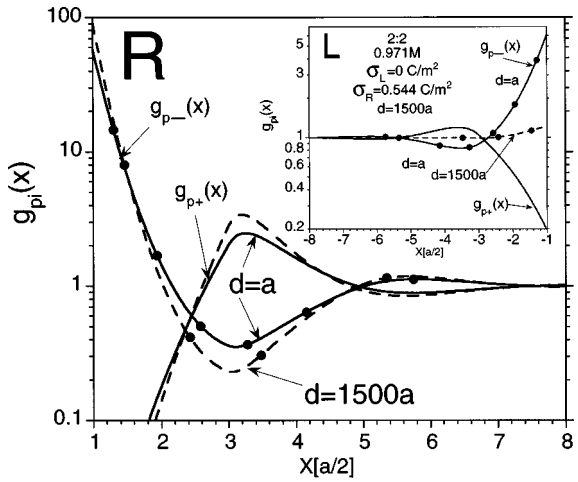

FIG. 3. Reduced concentration profiles for a 2:2, 0.971M electrolyte, next to a charged wall, as a function of the distance to the wall, in units of ionic radius. The wall has surface charge densities $\sigma_L = 0$ C/m^2 on its left surface and $\sigma_R = 0.544$ C/m^2 on its right surface. Two thicknesses of the wall are considered: $d = a$ (solid lines) and $d = 1500a$ (dashed lines). We show the PIRCP (plain lines) and the NIRCP (lines with filled circles). The distance to the wall is measured in ionic radius. The zero of the x coordinate is located on the left surface of the wall for the left RCPs and on the right surface of the wall for the right RCPs, i.e., the thickness of the wall is not plotted. The left RCPs are shown in the inset. The curves for the PIRCP and the NIRCP on the left-hand side of the $d = 1500a$ wall coincide.

Is the total charge induced in the liquid equal to the total charge on the wall? Is the fluid at the left and right of the wall at a constant chemical potential? If there is no liquid on, say, the right-hand side of the wall, how are the ionic profiles modified?

In Fig. 3 the fluid is a 2:2, 0.971M electrolyte and $\sigma_L = 0$ C/m^2 and $\sigma_R = 0.544$ C/m^2. Two thickness of the wall are considered: $d = a$ and $1500a$. For a wall thickness of $d = 1500a$, a physically appealing result is obtained on both sides of the wall, i.e., the PIRCP and the NIRCP near the wall are well above one at the left-hand side of the wall, whereas the NIRCP is higher than one and the PIRCP is lower than than one at the right-hand side of the wall. A calculation for a symmetrically charged wall [with Eq. (1)] or with traditional methods [7], with charge density equal to 0.544 C/m^2, shows a PIRCP and a NIRCP equal to those shown in Fig. 3 for the right-hand side of the wall. A similar result is observed from a calculation for a symmetrically charged wall, with charge density equal to 0 C/m^2, i.e., its NIRCP and PIRCP agree with those shown in Fig. 3 for the left-hand size of the $d = 1500a$ wall. On the other hand, it has been proved in the past that for a symmetrically charged plate the NIRCP and PIRCP are independent of the width of the plate [31,32]. Our calculations corroborate this fact. Thus, if for a symmetrically charged wall the concentration profiles are symmetrical and independent of the width of the wall and if these profiles are equal to the corresponding profiles next to a very thick unsymmetrically charged wall, then the differences in the profiles for narrow walls are due to a correlation between the liquids on the left- and right-hand sides of the wall.

Let us point out that although Eq. (2) is a wall-ion potential that increases with the value of $|x|$, measured from the center of the wall, at both sides of the wall, the left and right fluids become uncorrelated for large values of d. Therefore, the observed correlation is a true many-body effect and not a feature of the wall-ion potential.

Let us give another argument in support of this correlation between the liquids at both sides of a wall. Although we may be redundant, we believe the following argument could give a different, perhaps useful, perspective. In Fig. 3, at the left-hand side of the wall, the NIRCP and PIRCP coincide and are equal to those for the reduced concentration profile of a hard-sphere fluid (the $d = 1500$ case). This should be the result for our primitive model, where the positive and negative ions differ from each other only in their charge sign. Since the NIRCP and PIRCP at the left-hand side of the wall are on top of each other, the fluid at the right-hand side of the wall cannot ''see'' its charge, i.e., it is equivalent to having a vacuum at the left-hand side of the wall. On the other hand, as pointed out above, the RCPs at each side of a very thick, unsymmetrically charged wall are equal to those for symmetrically charged walls, charged with the corresponding charge. Hence, in Fig. 3 the right RCPs for the $d = 1500a$ case are equal to those for a very thick wall, symmetrically charged with 0.544 C/m^2. Therefore, it is clear that having a vacuum or a charged liquid at the left-hand side of a very thick wall has no effect on the liquid at the right-hand side of the wall. This shows, perhaps in a particularly clear way, that the liquids at both sides of a very thick wall are not correlated. Suppose now that we have a vacuum at the left-hand side of a *narrow* wall. Then, from Gauss's law, an ion at the right-hand side of the wall will see a sheet of charge with a surface charge density equal to $\sigma_R + \sigma_L$, say, equal to 0.544 C/m^2 [see Eq. (2)]. The result would be independent of the width of the wall since there is a vacuum at the left-hand side of the wall and the wall-ion potential is independent of the width of the wall [see Eq. (2)]. Thus the RCPs for a narrow wall, with a vacuum on one side, must be equal to those for a very thick wall, equally charged, and also with a vacuum on one side. Thus it is clear that the RCPs at the right-hand side of a narrow wall with a vacuum at its left-hand side will be equal to those shown in Fig. 3 for the right-hand side of the $d = 1500a$ wall. Therefore, in Fig. 3 the difference between the $d = a$ RCPs and those for the $d = 1500a$ RCPs is due to a correlation of the liquids at both sides of the wall.

In Fig. 4 the fluid is a 2:2, 0.971M electrolyte and $\sigma_L = -0.136$ C/m^2 and $\sigma_R = 0.68$ C/m^2. Two thicknesses of the wall are considered: $d = a$ and $5000a$. We show the PIRCP and NIRCP. In Fig. 5 the fluid is a 2:2, 0.05M electrolyte and $\sigma_L = -0.136$ C/m^2 and $\sigma_R = 0.68$ C/m^2. Two thicknesses of the wall are considered: $d = a$ and $500a$. We show the PIRCP and the NIRCP. In Fig. 6 the fluid is a 1:1, 0.1M electrolyte and $\sigma_L = -0.136$ C/m^2 and $\sigma_R = 0.68$ C/m^2. Two thicknesses of the wall are considered: $d = a$ and $1500a$. We show the PIRCP and the NIRCP. The results for the large values of d in Figs. 4–6 show that a lower charge or concentration of the salt produces thicker EDLs, i.e., the RCPs are of longer range and the counterion RCPs have higher contact values for a lower charge or concentration of the salt. This is to be expected since for large values of d we

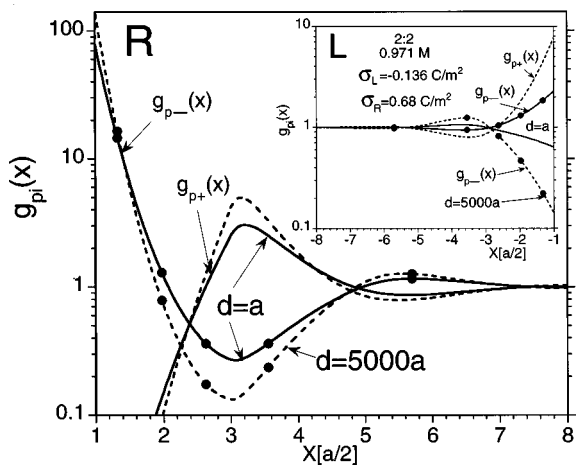

FIG. 4. Reduced concentration profiles for a 2:2, 0.971*M* electrolyte, next to a charged wall, as a function of the distance to the wall, in units of ionic radius. The wall has surface charge densities $\sigma_L = 0.136$ C/m^2 on its left surface and $\sigma_R = 0.68$ C/m^2 on its right surface. Two thicknesses of the wall are considered: $d = a$ (solid lines) and $d = 5000a$ (dashed lines). We show the PIRCP (plain lines) and the NIRCP (lines with filled circles). The distance to the wall is measured in units of ionic radius. The zero of the x coordinate is located on the left surface of the wall for the left RCPs and on the right surface of the wall for the right RCPs, i.e., the thickness of the wall is not plotted. The left RCPs are shown in the inset.

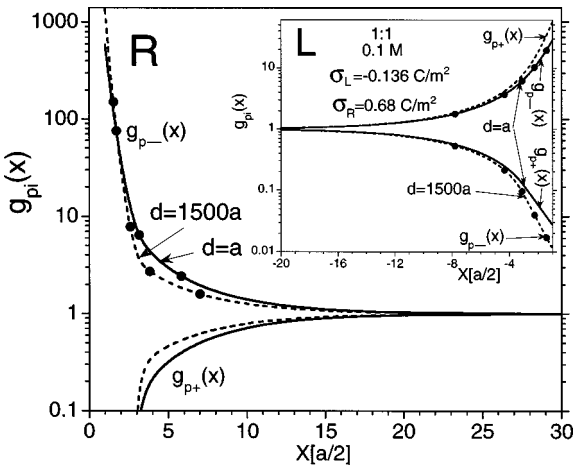

FIG. 6. Reduced concentration profiles for a 1:1, 0.1*M* electrolyte, next to a charged wall, as a function of the distance to the wall, in units of ionic radius. The wall has surface charge densities $\sigma_L = -0.136$ C/m^2 on its left surface and $\sigma_R = 0.68$ C/m^2 on its right surface. Two thicknesses of the wall are considered: $(d = a)$ (solid lines) and $d = 1500a$ (dashed lines). We show the PIRCP (plain lines) and NIRCP (lines with filled circles). The distance to the wall is measured in units of ionic radius. The zero of the x coordinate is located on the left surface of the wall for the left RCPs and on the right surface of the wall for the right RCPs, i.e., the thickness of the wall is not plotted. The left RCPs are shown in the inset.

recover the single EDL results and this is a well-known behavior for infinitely thick walls [7,35]. For $d = a$, this qualitative behavior of the EDL persist. However, a comparison of these results with the corresponding results for large values of d suggests that a thicker EDL implies a stronger correlation between the liquids on both sides of the wall; see, for example, the left NIRCP, where a lower charge or concentration of the salt produces larger deviations with respect the corresponding NIRCP for large values of d.

In Figs. 7 and 8 the fluid is a 2:2, 0.971*M* electrolyte and $\sigma_L = -0.136$ C/m^2 and $\sigma_R = 0.68$ C/m^2. Results for the mean electrostatic potential profile (MEPP), for wall thicknesses of

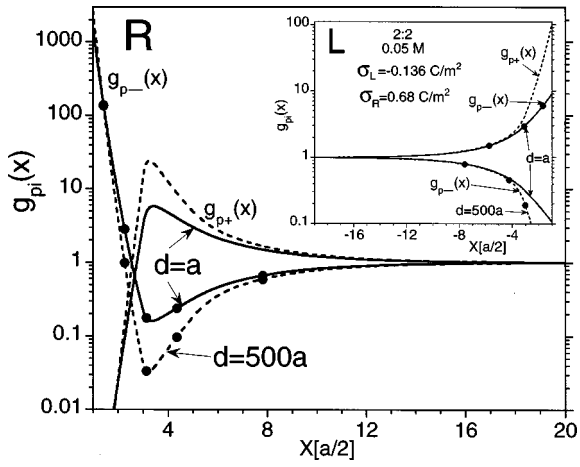

FIG. 5. Reduced concentration profiles for a 2:2, 0.05*M* electrolyte, next to a charged wall, as a function of the distance to the wall, in units of ionic radius. The wall has surface charge densities $\sigma_L = -0.136$ C/m^2 on its left surface and $\sigma_R = 0.68$ C/m^2 on its right surface. Two thicknesses of the wall are considered: $d = a$ (solid lines) and $d = 500a$ (dashed lines). We show the PIRCP (plain lines) and NIRCP (lines with filled circles). The distance to the wall is measured in units of ionic radius. The zero of the x coordinate is located on the left surface of the wall for the left RCPs and on the right surface of the wall for the right RCPs, i.e., the thickness of the wall is not plotted. The left RCPs are shown in the inset.

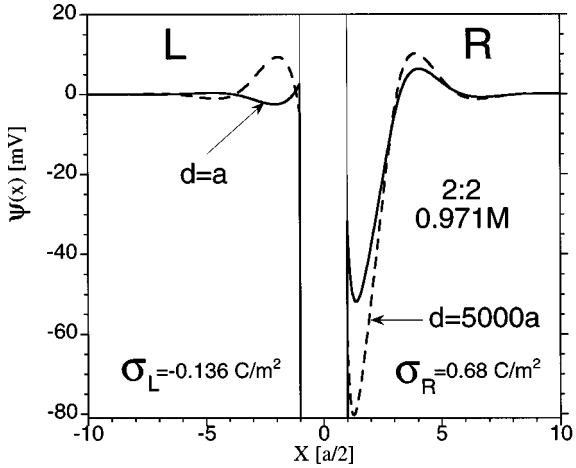

FIG. 7. Mean electrostatic potential profile (MEPP) for a 2:2, 0.971*M* electrolyte, next to a charged wall, as a function of the distance to the wall, in units of ionic radius. The wall has surface charge densities $\sigma_L = -0.136$ C/m^2 on its left surface and $\sigma_R = 0.68$ C/m^2 on its right surface. The thicknesses of the wall are $d = a$ (solid line) and $d = 5000a$ (dashed line). The distance to the wall is measured in units of ionic radius. The zero of the x coordinate is located on the left surface of the wall for the left RCPs and on the right surface of the wall for the right RCPs, i.e., the thickness of the wall is not plotted.

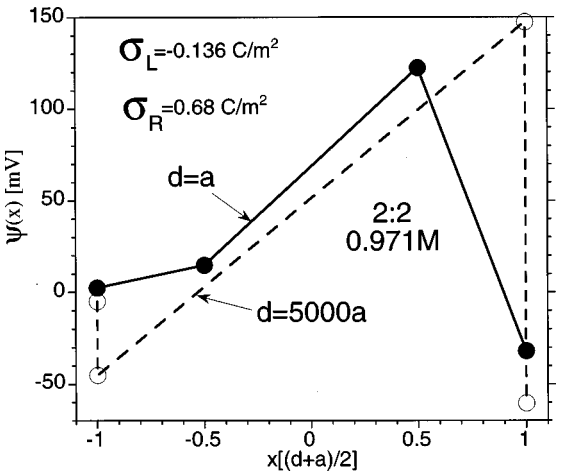

FIG. 8. MEPP inside a charged plate immersed in a 2:2, 0.971*M* electrolyte, as a function of the distance to the center of the wall, in units of $(d+a)/2$, where d is the wall thickness and a is the ionic diameter. The wall has surface charge densities $\sigma_L=-0.136$ C/m^2 on its left surface and $\sigma_R=0.68$ C/m^2 on its right surface. The thicknesses of the wall are $d=a$ (solid line) and $d=5000a$ (dashed line). The distance to the center of the wall is measured in units reduced by half the thickness of the wall plus half the ionic radius. The zero of the x coordinate is located at the center of the wall.

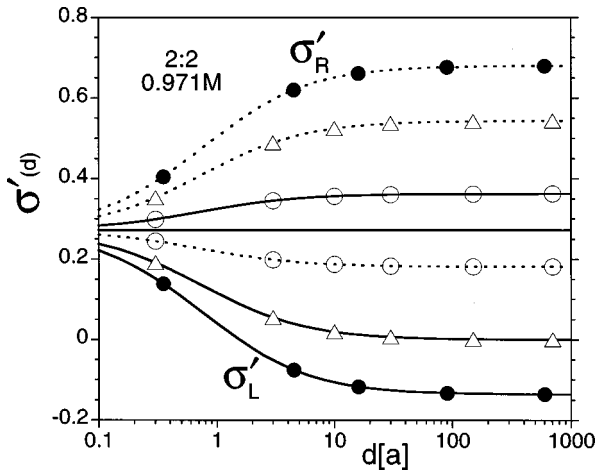

FIG. 9. Charge density induced in the fluid by the wall, as a function of the wall's thickness (measured in units of ionic diameter). The fluid is a 2:2, 0.971*M* electrolyte and the charge of the plate is the same as that in Fig. 2, i.e., (a) on its left surface $\sigma_L=0.272$ C/m^2 and on its right surface $\sigma_R=0.272$ C/m^2 (plain line); (b) $\sigma_L=0.3627$ C/m^2 and $\sigma_R=0.1813$ C/m^2 (lines with open circles); (c) $\sigma_L=0$ C/m^2 and $\sigma_R=0.544$ C/m^2 (lines with open triangles); (d) $\sigma_L=-0.136$ C/m^2 and $\sigma_R=0.68$ C/m^2 (lines with filled circles). In all cases $\sigma_R+\sigma_L=0.544$ C/m^2. σ'_L is the charge induced on the left-hand side of the wall, whereas σ'_R is that induced on the right-hand side of the wall: The solid lines are for σ'_L and the dashed lines are for σ'_R. For case (a) the solid and dashed lines coincide.

$d=a$ and $5000a$, are shown. In Fig. 7 the MEPP outside the wall is shown, whereas in Fig. 8 the MEPP for the region $-(a+d)/2<x<(a+d)/2$ is plotted. A comparison of the MEPP for $d=a$ and $5000a$ shows the effect of the correlation of the liquid at both sides of the wall on the MEPP. The derivative with respect to x of the MEPP gives the electrical field as a function of x. The effective electrical field at the left-hand side of the wall and for $d=a$ is less intense and has an opposite sign to that for $d=5000a$. This is consistent with the RCPs shown in Fig. 4: Near the wall, at the left-hand side, the PIRCP for $d=5000a$ and the NIRCP for $d=a$ are both above the bulk value and the PIRCP is much larger than the NIRCP. In the different regions plotted in Fig. 8 the electrical field is constant, i.e., the MEP has a linear dependence on x [see Eqs. (8)–(10)]. This is to be expected since in our model these regions obey the Laplace equation. It is seen that for $-1<x<-0.5$ the electrical field for $d=a$ has an opposite sign to that for $d=5000a$. This shows that the electrical field due to the liquid at the right-hand side of the $d=a$ wall is more intense than that produced by the surface charge on the left face of the wall. This is consistent with the concentration profiles shown in Fig. 4.

In Fig. 9 the charge density induced in the fluid by the wall, as a function of the wall's thickness (measured in units of ionic diameter), is plotted. The fluid is a 2:2, 0.971*M* electrolyte and the charge of the plate is the same as that in Fig. 2, i.e., (a) on its left surface $\sigma_L=0.272$ C/m^2 and on its right surface $\sigma_R=0.272$ C/m^2; (b) $\sigma_L=0.3627$ C/m^2 and $\sigma_R=0.1813$ C/m^2; (c) $\sigma_L=0$ C/m^2 and $\sigma_R=0.544$ C/m^2; (d) $\sigma_L=-0.136$ C/m^2 and $\sigma_R=0.68$ C/m^2. In all cases $\sigma_R+\sigma_L=0.544$ C/m^2. σ'_L is the charge induced on the left-hand side of the wall, whereas σ'_R is that induced on the right-hand side of the wall: For $d=0$, $\sigma'_L=\sigma'_R=0.272$ C/m^2; this is equal to the average charge on the wall. As d increases, σ'_L and σ'_R decrease or increase such that $\sigma'_L=\sigma_L$ and $\sigma'_R=\sigma_R$ for $d\to\infty$. In Fig. 9 it is seen that the total charge induced in the liquid, for all values of d, is equal to the total charge on the wall, i.e., there is overall electroneutrality. For very large values of d there is local electroneutrality, i.e., $\sigma'_L=\sigma_L$ and $\sigma'_R=\sigma_R$ for $d\to\infty$. However, for small values of d the left- and right-hand sides of the system are not independently electroneutral, i.e., $\sigma'_L\neq\sigma_L$ and $\sigma'_R\neq\sigma_R$. If we define $\Delta\sigma_L=|\sigma_L-\sigma'_L|$ and $\Delta\sigma_R=|\sigma_R-\sigma'_R|$, from Fig. 9 it can be seen that $\Delta\sigma_L=\Delta\sigma_R$ $(\equiv\Delta\sigma)$ for all four cases and for every value of d. This is to be expected if the total electroneutrality is conserved. For $d=0$ the wall becomes a sheet of charge, with a surface charge equal to $\sigma_L+\sigma_R$, i.e., the system becomes symmetric and the left RCPs become equal to their corresponding right RCPs. These RCPs are equal to those for an infinitely thick plate with a surface charge equal to half $\sigma_L+\sigma_R$. Therefore, the maximum of $\Delta\sigma$ is always for $d=0$, since for $d=0$

$$\sigma'_L=\sigma'_R=\frac{(\sigma_L+\sigma_R)}{2}. \tag{12}$$

The minimum of $\Delta\sigma$ is, of course, for $d\to\infty$, i.e., $\Delta\sigma=0$. From Fig. 9 it is clear that $\Delta\sigma$, as a function of d, has the same nonlinear behavior as that shown by σ'_L and σ'_R. Notice that $\Delta\sigma=0$ for all values of d, for case (a). For the other three cases, the $\Delta\sigma$ curves are higher for larger asymmetry in the charge between the left and right faces of the wall, i.e., $\Delta\sigma$ is the highest for case (d) and the lowest for case (b). The value of $\Delta\sigma$ is a measure of the violation of some sort of local electroneutrality condition [31,32,36,37] by the liquid at each side of the wall.

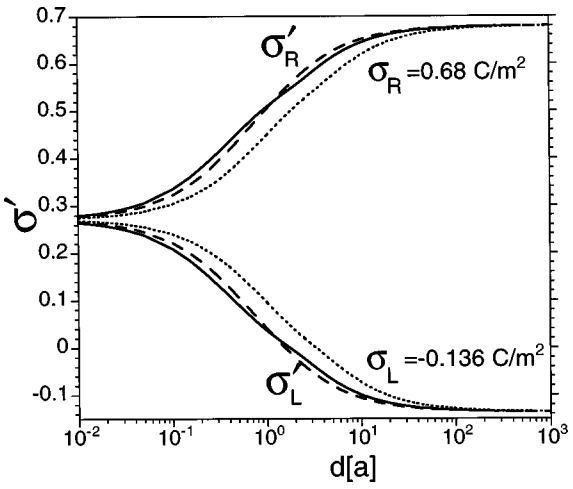

FIG. 10. Charge density induced in the fluid by the wall, as a function of the wall's thickness (measured in units of ionic diameter). The charge of the plate is $\sigma_L = -0.136\ \mathrm{C/m^2}$ and $\sigma_R = 0.68\ \mathrm{C/m^2}$. σ_L' is the charge induced on the left-hand side of the wall, whereas σ_R' is that induced on the right-hand side of the wall. The fluid is 2:2, 0.971M (dashed line); 2:2, 0.05M (solid line); and 1:1, 0.1M (dotted line).

If one takes this violation of the local electroneutrality condition as a measure of the correlation between the liquids on both sides of the wall, Figs. 2–4 and 9 show that there is a correlation of the liquid through the wall and that this is larger for larger asymmetries in the charge and smaller values of d.

In Fig. 10 the charge density induced in the fluid by the wall, as a function of the wall's thickness (measured in units ionic diameter), is shown. The charge of the plate is $\sigma_L = -0.136\ \mathrm{C/m^2}$ and $\sigma_R = 0.68\ \mathrm{C/m^2}$. σ_L' is the charge induced on the left-hand side of the wall, whereas σ_R' is that induced on the right-hand side of the wall. Different electrolytes are considered: (a) a 2:2, 0.971M electrolyte; (b) a 2:2, 0.05M electrolyte; and (c) a 1:1, 0.1M electrolyte. Clearly case (c) shows the lowest σ_R' (highest σ_L') for $0 < d < \infty$, i.e., the larger $\Delta\sigma$. Case (b) has a $\Delta\sigma$ smaller than that for case (a) for small values of d and larger than that for case (a) for large values of d. These results show a dependence of the correlation between the liquids at both sides of the wall with the thickness of the EDLs next to the wall. For large values of d we can say that, in general, a thicker EDL implies a stronger correlation. For small values of d, a higher concentration of the salt seems to produce a stronger correlation.

Figures 4–6, 9, and 10 show that the correlation between the liquids at both sides of the wall seems to increase with decreasing electrolyte charge and concentration. Hence there seems to be a higher correlation of the fluid, through the wall, for thicker EDLs. However, in the limit of zero charge the hard-sphere fluid is recovered, as expected for this model. All the data in Figs. 2–10 were obtained for $T = 298$ K, $\varepsilon = 78.5$, and $a = 4.25$ Å, which is the approximate size for a hydrated ion in solution, i.e., about two times the typical atomic diameter. For our $d = a$ case, perhaps one can think of a monolayer of polar diatomic molecules. In any case, we have chosen $d = a$ in Figs. 2–8 as an example of the correlation between the liquids on both sides of the wall. No particular significance is given to this particular value of the parameter d.

As pointed out in Sec. II, the sum rules proposed by Rosinberg, Blum, and Lebowitz [34] for the IPIM predict a net pressure different from zero, whereas in our case the pressure is zero. This difference is probably due to the fact that in their model the liquids on both sides of the interface are not correlated. In their model they do not have correlation through the wall because they forced the system to be, independently, electrically neutral at each side of the wall. In their case, for $d = 0$, they find unsymmetrical concentration profiles. In our case, for $d = 0$, the concentration profiles are symmetrical. This is puzzling since for $d = 0$ the system does not have a way of ''knowing'' what charge belongs to what side of the wall. In fact, since in Fig. 2 $\sigma_L + \sigma_R = 0.544\ \mathrm{C/m^2}$ for all four cases, for $d = 0$ the RCPs become equal to each other. We find our results, for our model, more physically appealing.

IV. CONCLUSION

The DM [27,28] is a general, simple method to derive integral equation theories for inhomogeneous fluids. This method is based on the recognition of the well-established equivalence between particles and fields. The AM [4,5] is a mathematical limit where clearly this principle is not recognized, since taking this limit is unnecessary. Hence the DM is more general than the AM, but it is not a generalization of it. There seems to be some confusion in the literature with regard to this point [29]. The AM can be applied only for infinitely thick planar walls. Perhaps due to the strong influence of the AM in the literature [7–17], no attention seems to have been given in the past to the relevant case of a wall of finite thickness. In this paper we have derived, through the DM, an integral equation for an inhomogeneous fluid next to a charged wall of *finite thickness*. We show that the liquids on the left- and right-hand sides of the wall are correlated. This correlation seems to be more important for thicker electrical double layers. The correlation disappears for infinitely thick walls. Thus, in the limit of infinitely thick walls we recover the well-established results for single electrical double layers [7–17,35].

By construction, the HNC-MSA equation for a plate immersed in a fluid, derived through the DM, is a theory for a constant chemical potential. That is, the fluids on both sides of the wall have the same chemical potential. However, although the total charge induced in the fluid cancels the total charge on the wall, each side of the system is not independently electroneutral. In Ref. [30] and in the present paper we have shown that is due to the correlation between the liquids on both sides of the wall. This correlation is a *many-body* effect. The ions at the, say, left-hand side of the wall interact among themselves, with those at the right-hand side of the wall, and with the wall. The result of all these interactions is an effective potential. The way in which this effective interaction goes from one side of the wall to the other and how it is modified by the wall's thickness is shown in Fig. 8.

In the past it has been shown that in confined fluids there is a violation of the local electroneutrality condition (LEC) [31,32,36,37]. That is, the fluid between two plates, *sym-*

metrically charged, does not cancel the charge on the inside surfaces of the plates. This violation of the LEC is larger for thinner plates and greater confinement. However, the LEC is satisfied for large separations between the plates and for any thickness of the plates. In this paper we report a violation of some sort of electroneutrality condition. However, here the fluid is not confined and the origin of this effect is due to a correlation of the fluid through the wall. As far as we know, this effect has not been recognized before and we believe it could be of far-reaching consequences in the field of statistical mechanics of condensed-matter systems, where boundaries between different kind of materials are present. In particular, this finding could be relevant in colloid, thin film, and biophysics studies.

In our calculations we have assumed the wall's dielectric constant to be equal to that of the solvent, to avoid image interactions. We have avoided image interactions to simplify our already elaborate system of nonlinear integral equations and to have a point of reference with most of the previous complex liquids literature, where image interactions are not taken into account [1–37]. However, the image interaction will probably enhance or decrease the correlation between the liquids on both sides of the wall if the wall's dielectric constant is lower or larger, respectively, than that of the solutions solvent. A low dielectric constant for the wall could be of interest for some biological systems. The fluid correlation through the wall need not be limited to a charged wall. This effect could be present, for example, in Lennard-Jones fluids next to a wall with surfaces with asymmetrical Lennard-Jones potentials.

ACKNOWLEDGMENT

We gratefully acknowledge the financial support of CONACYT, Grants Nos. 3163-E9307 and L0077-E9607.

[1] G. Gouy, J. Phys. A **9**, 457 (1910).
[2] D. L. Chapman, Philos. Mag. **25**, 475 (1913).
[3] F. H. Stillinger, Jr. and J. G. Kirkwood, J. Chem. Phys. **33**, 1282 (1960).
[4] D. Henderson, F. F. Abraham, and J. A. Barker, Mol. Phys. **31**, 1291 (1976).
[5] D. Henderson and L. Blum, J. Chem. Phys. **69**, 5441 (1978).
[6] S. Levine and C. W. Outhwaite, J. Chem. Soc. Faraday Trans. II **74**, 1670 (1978).
[7] M. Lozada-Cassou, R. Saavedra-Barrera, and D. Henderson, J. Chem. Phys. **77**, 5150 (1982), and references cited therein.
[8] P. V. Giaquinta and M. Parrinello, J. Chem. Phys. **81**, 4074 (1984).
[9] S. L. Carnie and G. M. Torrie, in *Advances in Chemical Physics*, edited by I. Prigogine and S. A. Rice (Wiley, New York, 1984).
[10] S. L. Carnie, Mol. Phys. **54**, 509 (1985), and references cited therein.
[11] C. W. Outhwaite and L. B. Bhuiyan, J. Chem. Phys. **84**, 3461 (1986), and references cited therein.
[12] P. Nielaba, T. Alts, B. D'Aguanno, and F. Fortsmann, Phys. Rev. A **34**, 1505 (1986), and references cited therein.
[13] M. Plischke and D. Henderson, J. Chem. Phys. **88**, 2712 (1988), and references cited therein.
[14] P. Attard, Phys. Rev. E **48**, 3604 (1993), and references cited therein.
[15] G. M. Torrie and J. P. Valleau, J. Chem. Phys. **73**, 5807 (1980).
[16] I. Snook and W. van Megen, J. Chem. Phys. **75**, 4104 (1981).
[17] B. Svensson, B. Jönsson, and C. E. Woodward, J. Phys. Chem. **94**, 2105 (1990).
[18] E. J. Verwey and J. Th. G. Overbeek, *Theory of Stability of Lyophobic Colloids* (Elsevier, Amsterdam, 1948).
[19] R. J. Hunter, *Zeta Potential in Colloid Science* (Academic, London, 1981).
[20] A. W. Adamson, *Physical Chemistry of Surfaces* (Wiley, New York, 1982).
[21] R. D. Vold and M. J. Vold, *Colloid and Interface Chemistry* (Addison-Wesley, London, 1983).
[22] P. C. Hiemenz, *Principles of Colloid and Surface Chemistry* (Dekker, New York, 1986).
[23] T. G. M. van de Ven, *Colloidal Hydrodynamics* (Academic, London, 1989).
[24] M. J. Rosen, *Surfactants and Interfacial Phenomena* (Wiley, New York, 1989).
[25] W. B. Russel, D. A. Saville, and W. R. Schowalter, *Colloidal Dispersions* (Cambridge University Press, Cambridge, 1989).
[26] K. S. Schmitz, *Macroions in Solution and Colloidal Suspensions* (VCH, New York, 1993).
[27] M. Lozada-Cassou, J. Chem. Phys. **75**, 1412 (1981); **77**, 5258 (1982).
[28] M. Lozada-Cassou, in *Fundamentals of Inhomogeneous Fluids*, edited by D. J. Henderson (Dekker, New York, 1992), Chap. 8.
[29] See, for example, P. Zaini, H. Modarress, and G. A. Mansoori, J. Chem. Phys. **104**, 3832 (1996).
[30] M. Lozada-Cassou and J. Yu, Phys. Rev. Lett. **77**, 4019 (1996).
[31] M. Lozada-Cassou, J. Chem. Phys. **80**, 3344 (1984).
[32] M. Lozada-Cassou and E. Díaz-Herrera, J. Chem. Phys. **92**, 1194 (1990).
[33] M. L. Rosinberg and L. Blum, J. Chem. Phys. **81**, 3700 (1984).
[34] M. L. Rosinberg, L. Blum, and J. L. Lebowitz, J. Chem. Phys. **83**, 892 (1985).
[35] See, for example, M. Lozada-Cassou and D. Henderson, J. Phys. Chem. **87**, 2821 (1983).
[36] M. Lozada-Cassou, W. Olivares, and B. Sulbarán, Phys. Rev. E **53**, 522 (1996).
[37] M. Lozada-Cassou, W. Olivares, B. Sulbarán, and Y. Jiang, Physica A **231**, 197 (1996).